

Five-body systems with Bethe-Salpeter equations

Gernot Eichmann^{1,*}, M.T. Peña^{2,3,†} and Raul D. Torres^{2,3,‡}

¹*Institute of Physics, University of Graz, NAWI Graz, Universitätsplatz 5, 8010 Graz, Austria*

²*Departamento de Física, Instituto Superior Técnico, Universidade de Lisboa, Av. Rovisco Pais 1, 1049-001 Lisboa, Portugal and*

³*Laboratório de Instrumentação e Física Experimental de Partículas, Av. Prof. Gama Pinto 2, 1649-003 Lisboa, Portugal*

(Dated: February 26, 2025)

We extend the Bethe-Salpeter formalism to systems made of five valence particles. Restricting ourselves to two-body interactions, we derive the subtraction terms necessary to prevent overcounting. We solve the five-body Bethe-Salpeter equation numerically for a system of five scalar particles interacting by a scalar exchange boson. To make the calculations tractable, we implement properties of the permutation group S_5 and construct an approximation based on intermediate two- and three-body poles. We extract the five-body ground and excited states along with the spectra obtained from the two-, three-, and four-body equations. In the limit of a massless exchange particle, the two-, three, four- and five-body states coexist within a certain range of the coupling strength, whereas for heavier exchange particles the five-body system becomes Borromean. Our study serves as a building block for the calculation of pentaquark properties using functional methods.

I. INTRODUCTION

There are presently five pentaquark candidates with minimal quark content $qqq\bar{c}\bar{c}$ (with $q = u, d, s$), which have been observed by the LHCb collaboration in the $J/\Psi p$ and $J/\Psi \Lambda$ invariant mass spectra [1–3]. The proximity of their peaks to meson-baryon thresholds suggests a molecular explanation in terms of meson-baryon molecules. This picture has been frequently employed in effective field theory and model calculations, in analogy to several exotic meson candidates in the charmonium sector, see e.g. [4–10].

In general, it is a highly interesting question how a state made of valence quarks and/or antiquarks transforms into a molecular state, given that quantum field theory does not provide the means to rigorously distinguish between these scenarios. In the analogous case of four-quark ($qq\bar{q}\bar{q}$) states, one way to identify such a mechanism is the Bethe-Salpeter equation (BSE) [11–13]: In its solution, the four-quark wave function dynamically develops two-body clusters in the form of meson-meson and diquark-antidiquark configurations. For baryons with three valence quarks, the analogue is the formation of internal diquark clusters [14, 15]. In the case of pentaquarks, the internal clusters are mesons and baryons, which naturally leads to molecular configurations in the vicinity of meson-baryon thresholds.

Motivated by these ideas, in the present work we extend the Bethe-Salpeter formalism [16–19] to five-body systems. As a first application we consider the massive Wick-Cutkosky model [20–22], which describes the interactions of scalar particles through scalar exchanges. The applications of the two-body BSE in this model are well

explored by now [22–39] and the three-body BSE has been investigated in [40–42]. In the present study we extend this approach to also calculate the spectrum of four- and five-body states.

The paper is organized as follows. In Sec. II we establish the five-body BSE and derive the subtraction terms for the two-body kernel that are necessary to avoid overcounting. We discuss approximations based on the multiplet structure of the permutation group S_5 [43] and the emergence of internal two- and three-body poles. In Sec. III we present our results, and we conclude in Sec. IV. Appendix A collects technical details on n -body BSEs. We employ a Euclidean metric throughout this work, see [14] for conventions.

II. FIVE-BODY EQUATION

A. General form of the BSE

Our starting point is the homogeneous BSE for a five-body system shown in Fig. 1:

$$\Gamma^{(5)} = K^{(5)} G_0^{(5)} \Gamma^{(5)}. \quad (1)$$

Here, $K^{(5)}$ is the five-body interaction kernel which consists of two-, three-, four- and five-body interactions, $G_0^{(5)}$ is the product of five dressed particle propagators, and $\Gamma^{(5)}$ is the five-body Bethe-Salpeter amplitude. In this compact notation, each multiplication represents an integration over all four-momenta in the loops.

Like any other homogeneous BSE, the five-body BSE can be derived from the pole behavior of the 5-body scattering matrix $T^{(5)}$, which is a ten-point correlation function and satisfies the scattering equation

$$T^{(5)} = K^{(5)} + K^{(5)} G_0^{(5)} T^{(5)}. \quad (2)$$

* gernot.eichmann@uni-graz.at

† teresa.pena@tecnico.ulisboa.pt

‡ raul.torres@tecnico.ulisboa.pt

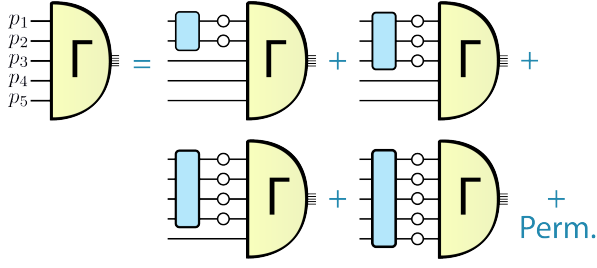


FIG. 1. Five-body Bethe Salpeter equation with two-, three-, four- and five-body kernels.

At a given bound-state or resonance pole with mass M , it assumes the form

$$T^{(5)} \longrightarrow \frac{\Gamma^{(5)} \bar{\Gamma}^{(5)}}{P^2 + M^2}, \quad (3)$$

where $\bar{\Gamma}^{(5)}$ is the charge-conjugate amplitude. Comparing the residues on both sides of the equation yields the homogeneous equation (1).

In the following we neglect irreducible three-, four- and five-body forces, so that the resulting kernel consists of irreducible two-body interactions only. We will denote this two-body kernel by K and assume that $K^{(5)} \approx K$.

B. Subtraction diagrams

Like in the case of the four-body equation [44–46], a naive summation of two-body kernels leads to overcounting in Eq. (2) and one needs subtraction terms. In a five-body system there are ten possible two-body kernels

$$K_a \in \{K_{12}, K_{13}, K_{14}, K_{15}, K_{23}, K_{24}, K_{25}, K_{34}, K_{35}, K_{45}\}, \quad (4)$$

where the indices label the valence particles, and 15 independent double-kernel configurations of the form

$$K_a K_b \in \{K_{12} K_{34}, K_{12} K_{35}, K_{12} K_{45}, K_{13} K_{24}, K_{13} K_{25}, K_{13} K_{45}, K_{14} K_{23}, K_{14} K_{25}, K_{14} K_{35}, K_{15} K_{23}, K_{15} K_{24}, K_{15} K_{34}, K_{23} K_{45}, K_{24} K_{35}, K_{25} K_{34}\}. \quad (5)$$

By contrast, in a four-body system there are only six two-body kernels and three double-kernel configurations.

If we now define

$$K_1 := \sum_a^{10} K_a, \quad K_2 := \sum_{a \neq b}^{15} K_a K_b, \quad (6)$$

one can show that the combination

$$K = K_1 - K_2 \quad (7)$$

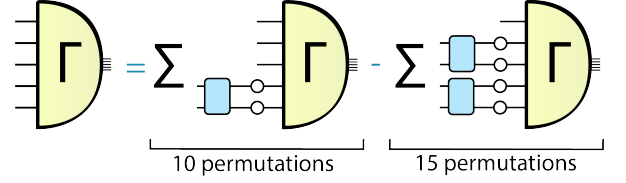


FIG. 2. Five-body BSE with two-body kernels and their subtraction terms as given in Eq. (7).

is free of overcounting, i.e., each possible monomial of the K_a appears exactly once and with coefficient 1 in the scattering matrix $T^{(5)} = K + K^2 + K^3 + \dots$ that follows from Eq. (2) by iteration, where we suppressed the propagator factors $G_0^{(5)}$ for brevity. The resulting equation is shown in Fig. 2.

Eq. (7) can also be derived as follows. We define the complementary three-body kernel $K_{a'}$ for a given two-body kernel K_a as

$$\begin{aligned} a = 12 : \quad K_{a'} &= K_{345} = K_{34} + K_{35} + K_{45}, \\ a = 13 : \quad K_{a'} &= K_{245} = K_{24} + K_{25} + K_{45}, \end{aligned} \quad (8)$$

and so on. Now suppose all interactions between the subsystems a and a' (say, $a = 12$ and $a' = 345$) were switched off. In that case, the full correlation function $G^{(5)} = G_0^{(5)} + G_0^{(5)} T^{(5)} G_0^{(5)}$ must factorize into the product $G_a G_{a'}$. Suppressing again the propagators in the notation, we have

$$G^{(5)} = 1 + T^{(5)} \stackrel{!}{=} G_a G_{a'} = (1 + T_a)(1 + T_{a'}) \quad (9)$$

$$\Rightarrow T^{(5)} = T_a + T_{a'} + T_a T_{a'}. \quad (10)$$

Here, T_a and $T_{a'}$ are the scattering matrices for the two- and three-body subsystems, which satisfy scattering equations analogous to Eq. (2) (written symbolically):

$$\begin{aligned} T_a &= K_a (1 + T_a) = \frac{K_a}{1 - K_a}, \\ T_{a'} &= K_{a'} (1 + T_{a'}) = \frac{K_{a'}}{1 - K_{a'}}. \end{aligned} \quad (11)$$

Plugging Eq. (11) into (10) yields

$$T^{(5)} = K (1 + T^{(5)}) = \frac{K}{1 - K} \quad (12)$$

with K given by $K = K_a + K_{a'} - K_a K_{a'}$. This is just Eq. (7) if the interactions between the clusters (12) and (345) are switched off, because in that case the kernels K_1 and K_2 in Eq. (6) reduce to

$$\begin{aligned} K_1 &= K_{12} + K_{34} + K_{35} + K_{45}, \\ K_2 &= K_{12} (K_{34} + K_{35} + K_{45}) \end{aligned} \quad (13)$$

and therefore $K_1 - K_2 = K_a + K_{a'} - K_a K_{a'}$ for $a = 12$ and $a' = 345$. Since this relation holds for any combination of clusters aa' , Eq. (7) is the full two-body kernel.

We also note a subtle difference compared to the four-body equation. In that case, Eq. (7) contains six single-kernel terms and three double-kernel subtraction terms. This can also be written as the sum over three topologies (12)(34), (13)(24) and (14)(23), where each contribution is given by $K_a + K_{a'} - K_a K_{a'}$ (e.g., $K_{12} + K_{34} - K_{12} K_{34}$). In the five-body case this cannot be directly taken over due to the different meaning of K_a and $K_{a'}$. However, it is still possible to define a kernel $K_{aa'}$ for each single two-body topology in Eq. (4) such that

$$K = \sum_{aa'}^{10} K_{aa'} \quad (14)$$

is the sum over the ten topologies. To this end, we define

$$K_3 := \sum_{a'}^{10} K_{a'}, \quad K_4 := \sum_{aa'}^{10} K_a K_{a'}. \quad (15)$$

Because each $K_{a'}$ is the sum of three two-body kernels, and because K_1 and K_2 contain 10 and 15 terms, respectively, this entails $K_3 = 3K_1$ and $K_4 = 2K_2$. Thus we can write the full two-body kernel K as

$$K = K_1 - K_2 = \alpha K_1 + (1 - \alpha) \frac{K_3}{3} - \frac{K_4}{2}, \quad (16)$$

where α is an arbitrary parameter. Each contribution is now a sum over 10 terms, so one can read off the single-topology kernel $K_{aa'}$ in Eq. (14). For example, choosing $\alpha = 1$ yields $K_{aa'} = K_a - K_a K_{a'}/2$, whereas $\alpha = \frac{1}{4}$ gives

$$K_{aa'} = \frac{K_a}{4} + \frac{K_{a'}}{4} - \frac{K_a K_{a'}}{2}. \quad (17)$$

C. Explicit form of the BSE

To write down the explicit form of the five-body equation, we consider a scalar system made of five scalar particles; the generalization to particles with spin is straightforward. The Bethe-Salpeter amplitude $\Gamma(\{p_i\})$ in Fig. 1 depends on five momenta $p_1 \dots p_5$, whose sum is the total onshell momentum P with $P^2 = -M^2$. According to Eq. (7) and Fig. 2, the five-body equation can be written as

$$\Gamma(\{p_i\}) = \sum_a^{10} \Gamma_{(a)}(\{p_i\}) - \sum_{a \neq b}^{15} \Gamma_{(a,b)}(\{p_i\}), \quad (18)$$

where $\Gamma_{(a)}(\{p_i\})$ is the diagram with a two-body kernel attached to the particle pair $a = (a_1, a_2)$ from Eq. (4), and $\Gamma_{(a,b)}(\{p_i\})$ is the diagram with two kernels attached to the pairs $a = (a_1, a_2)$ and $b = (b_1, b_2)$ from Eq. (5):

$$\begin{aligned} \Gamma_{(a)}(\{p_i\}) &= \int \frac{d^4 r}{(2\pi)^4} K(p_{a_1}, q_{a_1}, p_{a_2}, q_{a_2}) \\ &\quad \times D(q_{a_1}) D(q_{a_2}) \Gamma(\{p_i\}, a), \\ \Gamma_{(a,b)}(\{p_i\}) &= \int \frac{d^4 r}{(2\pi)^4} K(p_{a_1}, q_{a_1}, p_{a_2}, q_{a_2}) \\ &\quad \times D(q_{a_1}) D(q_{a_2}) \Gamma_{(b)}(\{p_i\}, a). \end{aligned} \quad (19)$$

Here, $K(p_{a_1}, q_{a_1}, p_{a_2}, q_{a_2})$ are the two-body kernels and $D(p^2)$ the single-particle propagators. The particle momenta inside the loop, where r is the exchanged four-momentum, are given by

$$q_{a_1} = p_{a_1} - r, \quad q_{a_2} = p_{a_2} + r. \quad (20)$$

The amplitudes inside the loop are

$$\Gamma(\{p_i\}, a) = \Gamma(p_1, \dots, q_{a_1}, \dots, q_{a_2}, \dots, p_5), \quad (21)$$

where p_{a_1} is replaced by q_{a_1} and p_{a_2} by q_{a_2} .

In practice it is useful to work with the total momentum P and four relative momenta q, p, k, l instead of the five particle momenta p_i with $i = 1 \dots 5$. To this end, we employ the momenta

$$\begin{aligned} q &= \frac{p_1 - p_5}{2}, & p &= \frac{p_2 - p_5}{2}, \\ k &= \frac{p_3 - p_5}{2}, & l &= \frac{p_4 - p_5}{2}. \end{aligned} \quad (22)$$

The amplitude $\Gamma(q, p, k, l, P)$ then depends on 15 Lorentz invariants that can be formed from these momenta, namely

$$\begin{aligned} q^2, & \quad \omega_1 = q \cdot p, \\ p^2, & \quad \omega_2 = q \cdot k, & \eta_1 &= q \cdot P, \\ k^2, & \quad \omega_3 = q \cdot l, & \eta_2 &= p \cdot P, \\ l^2, & \quad \omega_4 = p \cdot k, & \eta_3 &= k \cdot P, \\ P^2, & \quad \omega_5 = p \cdot l, & \eta_4 &= l \cdot P, \\ & \quad \omega_6 = k \cdot l, \end{aligned} \quad (23)$$

These can be arranged into multiplets of the permutation group S_5 , namely two singlets, two quartets and a quintet [43]. The singlet variables are

$$\mathcal{S}_0 = \frac{1}{5} \left(q^2 + p^2 + k^2 + l^2 - \frac{1}{2} \sum_{i=1}^6 \omega_i \right) \quad (24)$$

and $P^2 = -M^2$. One quartet is constructed from the angular variables η_i , and the remaining variables are distributed over a quartet and a quintet. In four spacetime dimensions there is an additional relation between these 15 variables so that only 14 are independent. In practice this leads to a nontrivial relation between the quintets, quartets and singlets which involves five powers in the variables (23), see Appendix D of Ref. [43] for details.

Table I shows the extension of the multiplet construction to general n -body systems, which are subject to the permutation group S_n [43]. For any n one can construct a singlet \mathcal{S}_0 analogous to Eq. (24), and P^2 is always a singlet. A general n -body system has $n - 1$ relative momenta and hence $n - 1$ angular variables η_i , which form an $(n - 1)$ -dimensional multiplet of S_n . The variables $p_1^2 \dots p_n^2$ form another $(n - 1)$ -plet, with their sum being constrained by \mathcal{S}_0 . In total there are $n(n + 1)/2$

n	S_0	P^2	η_i	$p_1^2 \dots p_n^2$	\mathcal{M}	Total	Indep.
2	1	1	1	—	—	3	3
3	1	1	2	2	—	6	6
4	1	1	3	3	2	10	10
5	1	1	4	4	5	15	14
6	1	1	5	5	9	21	18
n	1	1	$n-1$	$n-1$	$n(n-3)/2$	$n(n+1)/2$	$4n-6$

TABLE I. S_n multiplet counting for an n -body system [43], see text for the discussion.

Lorentz invariants, so the difference $n(n-3)/2$ gives another multiplet (denoted by \mathcal{M} in Table I). For example, a two-body system forms two singlets (q^2 and P^2) and an antisinglet ($q \cdot P$). A three-body system gives two singlets (S_0 and P^2) and two doublets [47, 48], and a four-body system two singlets (S_0 and P^2), a doublet and two triplets [49]. For five-body systems one also encounters for the first time the dimensional constraint relating the Lorentz invariants, because n four-vectors can only depend on $4n-6$ independent variables.

While a system depending on such a large number of variables is extremely costly to solve numerically, the S_n construction allows one to switch off entire multiplets without affecting the symmetries of the system. This is especially useful for constructing approximations where one singles out the multiplets with the largest impact on the dynamics. Previous solutions of two-, three- and four-body systems show that the dependence on the angular variables η_i is usually small or even negligible [11]. Similarly, Bose-symmetric n -point functions like the three- and four-gluon vertex, which are obtained from Table I by setting $P^2 = 0$ and all $\eta_i = 0$, show a planar degeneracy and depend mainly on S_0 [47, 50–53].

The crucial observation from four-body systems is that the BSE dynamically generates intermediate two-body poles in the solution process. Specifically, a four-quark ($qq\bar{q}\bar{q}$) equation in QCD produces intermediate meson (and diquark) poles and thus dynamically creates resonance channels. In the four-body system these poles only appear in the doublet \mathcal{M} , so that the dynamics is largely determined by S_0 and \mathcal{M} . In a five-body system, on the other hand, there are 10 possible two- and three-body configurations $aa' = (12)(345), (13)(245), \dots$ which are distributed over the quartet and quintet. Together with S_0 , one would thus still need to include 10 variables in the BSE to capture the important dynamics.

Given that the leading momentum dependence of the amplitude beyond the singlet variable S_0 comes from the two-body and three-body clusters, here we follow a more efficient strategy that has been developed in the four-body case [13, 54, 55]: We reduce the momentum dependence to S_0 but include the two- and three-body poles explicitly. The resulting amplitude then reads

$$\Gamma(q, p, k, l, P) \approx f(S_0) \sum_{aa'} \mathcal{P}_{aa'}, \quad (25)$$

where e.g. for $aa' = (12)(345)$ the two- and three-body poles of the amplitude are given by

$$\mathcal{P}_{(12)(345)} = \frac{1}{(p_1 + p_2)^2 + M_M^2} \frac{1}{(p_3 + p_4 + p_5)^2 + M_B^2}.$$

Here, M_M and M_B are the masses of the two- and three-body subsystems (‘mesons’ and ‘baryons’), respectively. When plugging this ansatz into the five-body equation (18–19), the resulting dressing function $f(S_0)$ depends only on S_0 . In this way, the pole ansatz effectively captures the dependence on the remaining variables which is dominated by these poles.

In turn, this procedure requires knowledge of the bound-state masses M_M, M_B of the two- and three-body equations in the same approach. We solve these equations in a sequence by employing tree-level propagators for scalar constituent particles with mass m and a ladder approximation for a boson exchange with mass μ :

$$D(p) = \frac{1}{p^2 + m^2}, \quad K(p_{a_1}, q_{a_1}, p_{a_2}, q_{a_2}) = \frac{g^2}{r^2 + \mu^2}, \quad (26)$$

where r is the exchange momentum according to Eq. (20). We consider equal constituent masses for simplicity, but the generalization to unequal-mass systems is straightforward. In the following we employ a dimensionless coupling constant c and mass ratio β via

$$c = \frac{g^2}{(4\pi m)^2}, \quad \beta = \frac{\mu}{m}, \quad (27)$$

so that all results only depend on c and β while the mass m drops out.

The details on the two-, three-, four- and five-body equations for the scalar theory are provided in App. A. In the following we distinguish three approximations when solving these n -body equations. A ‘full solution’ refers to solving the respective BSE without any further approximations on the kinematics in the amplitude. At present, this is numerically only feasible for the two- and three body equations. The ‘singlet \times pole’ approximation refers to Eq. (25), with explicit two- and three-body poles for the five-body equation (‘mesons’ and ‘baryons’), and two-body poles for the three- and four-body equations (‘mesons’ or ‘diquarks’). Finally, the ‘singlet approximation’ refers to Eq. (25) without a pole ansatz, i.e., $\Gamma(q, p, k, l, P) \approx f(S_0)$, which will be used for comparisons.

III. RESULTS

In the following we present our solutions of the two-, three-, four- and five-body equations in the setup described above. In practice the BSEs turn into eigenvalue equations of the form

$$\lambda_i(P^2) \Psi_i(P^2) = \mathcal{K}(P^2) \Psi_i(P^2), \quad (28)$$

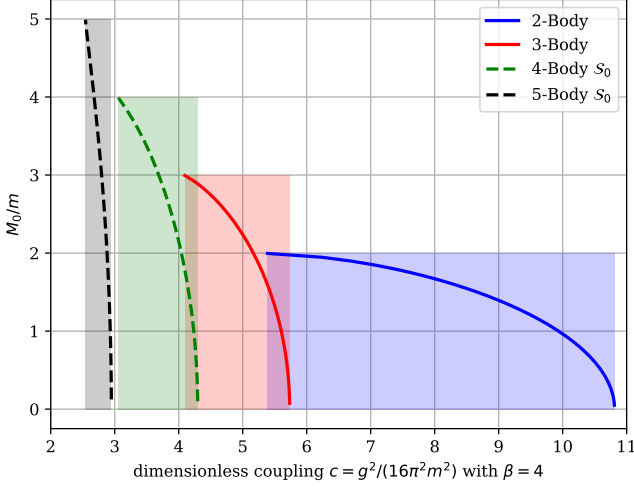


FIG. 3. Ground-state masses obtained from the n -body BSEs for $\beta = 4$ and different values of the coupling c . The two- and three-body results (solid curves) are full solutions, while the four- and five-body results (dashed curves) are obtained in the singlet approximation. The squares show the regions where ground-state solutions are possible.

where $P^2 \in \mathbb{C}$ is the total five-body momentum squared, $\mathcal{K}(P^2)$ is the kernel and the $\Psi_i(P^2)$ are its eigenvectors with eigenvalues $\lambda_i(P^2)$ for the ground ($i = 0$) and excited states ($i > 0$). If the condition $\lambda_i(P^2) = 1$ is satisfied, this corresponds to a pole in the scattering matrix at $P^2 = -M_i^2$ and determines the respective mass M_i . All results depend on two parameters, the coupling strength c and the mass ratio β . We cross-checked our results with the literature; our two-body solutions agree with those obtained in Refs. [31, 37] and our three-body solutions with those in Ref. [40].

Fig. 3 shows the variation of the ground-state masses M_0 obtained from the two-, three-, four- and five-body equations with the coupling strength c at a fixed value $\beta = 4$. One can see that for each system a ground state only exists within a certain range of the coupling. If the binding is too weak, the mass exceeds the respective threshold, and the bound state will turn into a resonance or virtual state on the second Riemann sheet. If the binding is too strong, the squared mass M_0^2 becomes negative and the bound state turns into a tachyon (see [37] for explicit examples). The latter property is presumably an artifact of the ladder approximation: Because the propagators remain at tree level and the three-point interaction vertices are constant, the coupling strength c only enters as an overall factor on each ladder kernel. In more advanced truncations where the n -point functions in the kernel are solved from their Dyson-Schwinger equations, the masses $M_i(c)$ would eventually approach constant values; see [56] for a corresponding study of the scalar two-body equation.

The lower coupling limit, below which the states become unbound, implies that below certain values of c not

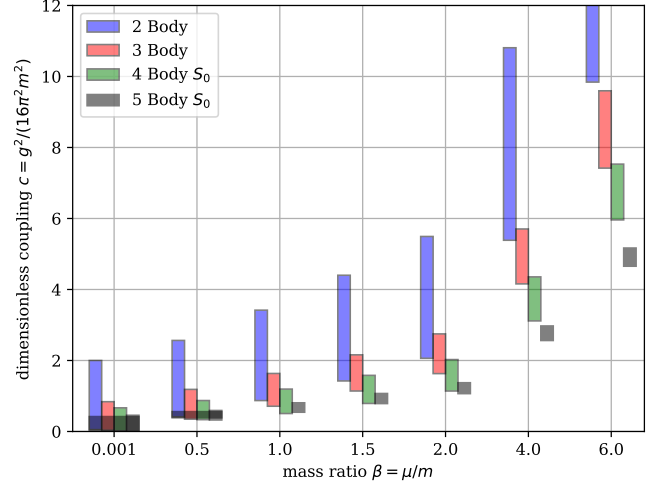


FIG. 4. Coupling ranges where n -body ground states are possible shown for different values of β . The horizontal displacement is for better readability. The color coding is the same as in Fig. 3. The black rectangles for small β values are the regions where all solutions coexist.

all ground states can coexist. For example, in Fig. 3 the three-body equation displays a Borromean behavior for $c \lesssim 5.5$, i.e., it admits a ground state while there is no corresponding two-body ground state. Similarly, for $c \lesssim 3$ the five-body equation admits a ground state while there are no two-, three- or four-body ground states. Fig. 4 displays the resulting coupling ranges for varying values of β . The coexistence regions are shown by the black rectangles and only exist for small β values ($\beta \lesssim 0.5$). For higher values of β the five-body system becomes Borromean, i.e., there is a five-body ground state without corresponding two- and three-body ground states.

In Fig. 5 we also show the radially excited states $M_{i>0}$ from the three-, four- and five-body solutions. For the extraction of the excited states we use an implementation of the Arnoldi algorithm [57].

As a consequence of the Borromean behavior, the five-body equation can dynamically generate two- and three-body ground-state poles only in the coexistence region. Outside this region, these poles would correspond to resonances or virtual states. Thus, the pole ansatz (25) can also only be sensibly applied in the coexistence region, which is why in Figs. 3, 4 and 5 we used the singlet approximation for the four- and five-body equations.

To go beyond this approximation, we must choose values of β and c inside the coexistence region. This is done in Fig. 6 for $\beta = c = 0.5$. Here we plot the inverse ground-state eigenvalues $1/\lambda_0(P^2)$ of the two-, three-, four- and five-body BSEs as a function of M (corresponding to $P^2 = -M^2$). We divide the mass by the sum of the propagator masses, such that the threshold of each equation is $\eta := M/\sum_i m_i = 1$. The ground-state masses M_0 are then obtained from the intersections $\lambda_0(P^2) = 1$. As before, the solid curves are the

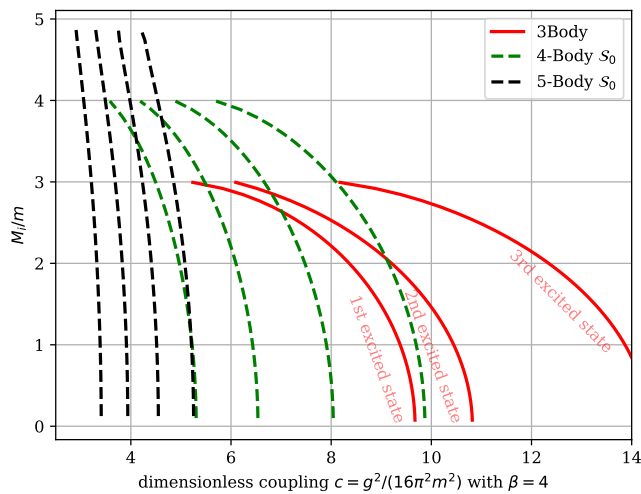


FIG. 5. Radially excited state masses $M_{i>0}$ for $\beta = 4$ and different values of the coupling c . The three-body results (solid curves) are full solutions, while the four- and five-body results (dashed curves) are obtained in the singlet approximation.

results from the full solutions (which are available for the two- and three-body BSEs). The dotted curves now correspond to the singlet approximation and the dashed curves to the singlet \times pole approximation. From the three-body curves one can see that the singlet \times pole approximation nicely agrees with the full solution, as long as the mass is not too far from the threshold, while the mass obtained with the singlet approximation is lower. The singlet \times pole ansatz is therefore a very good approximation of the dynamics in the system. The analogous observation in QCD is diquark clustering: The solution of the three-body Faddeev equation dynamically generates diquark poles, which dominate the behavior of the system, and the spectra and form factors in the quark-diquark approach agree well with those of the three-body solution [14, 15]. Likewise, four-quark ($qq\bar{q}\bar{q}$) systems dynamically generate meson and diquark poles which dominate their properties [11–13].

The vertical bands in Fig. 6 show the intersections of the eigenvalue curves with 1 for the singlet and singlet \times pole approximations. The resulting masses differ by $\lesssim 10\%$, so that already the singlet approximation yields reasonable estimates for them. However, this observation does not translate well to QCD; e.g., for light scalar $qq\bar{q}\bar{q}$ systems which are dominated by $\pi\pi$ channels, the singlet and singlet \times pole approximations lead to very different results due to the small pion mass [11].

Because the five-body equation dynamically generates two- and three-body poles, which is made explicit by the singlet \times pole approximation, this also lowers the threshold of the system from $M = 5m$ to $M = M_M + M_B$, where M_M is the ‘meson’ and M_B the ‘baryon’ mass. For the parameter values in Fig. 6 this leads to the restriction $\eta \lesssim 0.8$. Above this value, the five-body ground state turns into a resonance or virtual state, and one would

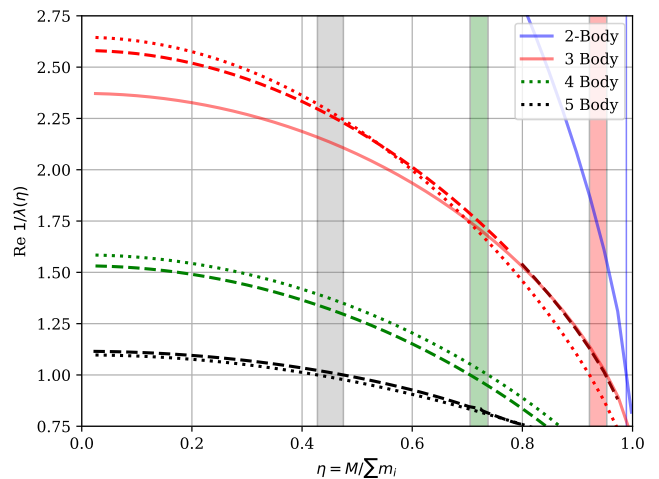


FIG. 6. Eigenvalues of the n -body BSEs for $\beta = c = 0.5$. Solid curves correspond to full solutions, dotted curves to the singlet approximation and dashed curves to the singlet \times pole approximation. The vertical bands show the resulting mass ranges when going from the singlet to the singlet \times pole approximation.

need to employ contour deformations and analytic continuations to extract its mass [37, 58]. Likewise, in the four-body system the threshold changes from $M = 4m$ to $M = 2M_M$, and in the three-body system it changes from $M = 3m$ to $M = m + M_M$.

Finally, in Fig. 7 we show the analogous eigenvalue plot for $\beta \approx 0$ corresponding to the massless Wick-Cutkosky model. With our definition (27) of the coupling strength, the inverse eigenvalues of the two-body system for $c = 1$ and $M = 0$ become integers, which can also be determined analytically [21, 31]. For the three-, four- and five-body systems, on the other hand, this does not appear to be the case.

IV. SUMMARY

We developed the five-body Bethe-Salpeter formalism and solved the five-body equation for a scalar model in a ladder truncation. The five-body Bethe-Salpeter amplitude depends on 14 momentum variables, which can be arranged in multiplets of the permutation group S_5 . To reduce this large number of variables, we employed an approximation in terms of two- and three-body poles, which the full amplitude would generate dynamically. Since this requires knowledge of the two- and three-body bound state masses, we also solved the corresponding two-, three- and four-body equations in the same approach. The two- and three-body equations can be solved without any approximations on the amplitude, and we find that a pole approximation in the three-body sector works very well. The approach developed in this work can be extended to QCD in view of investigating pentaquarks, and work in this direction is underway.

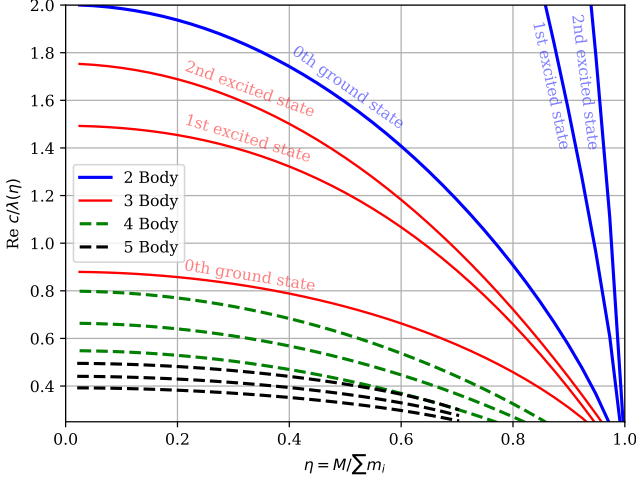


FIG. 7. BSE eigenvalues for $\beta = 0.001$, with $c = 1/4$ to ensure coexisting solutions for the two-, three-, four- and five-body BSEs (see Fig. 4). We rescaled the y axis again with c so that the condition $1/\lambda_i = 1$ for the physical solutions becomes $c/\lambda_i = 1/4$, which is the baseline in the plot. The two- and three-body results (solid curves) are full solutions, while the four- and five-body results (dashed curves) are obtained in the singlet \times pole approximation.

ACKNOWLEDGMENTS

We are grateful to Eduardo Ferreira and Joshua Hoffer for helpful discussions. This work was supported by the Portuguese Science fund FCT under grant numbers CERN/FIS-PAR/0023/2021 and PRT/BD/152265/2021 and by the Austrian Science Fund FWF under grant number 10.55776/PAT2089624. This work contributes to the aims of the USDOE ExoHad Topical Collaboration, contract DE-SC0023598.

Appendix A: n -body equations

In this appendix we provide details on the scalar three-, four- and five-body BSEs. An n -body bound state with total four-momentum P is the solution of the n -body BSE:

$$\Gamma^{(n)} = K^{(n)} G_0^{(n)} \Gamma^{(n)}. \quad (\text{A1})$$

We restrict ourselves to two-body interactions, so that $K^{(n)}$ is the sum of all two-body kernels (possibly including subtraction terms) and $G_0^{(n)}$ the product of the single-particle propagators. Using the one-boson exchange kernel in Eq. (26), the r.h.s. of each BSE can be written as the sum over the two-body interaction diagrams, where each contains a four-momentum integration over the exchange-boson momentum r , cf. Eq. (20). The explicit solution method for the two-body case can be found in Ref. [37]; in the following we discuss the three-, four- and five-body BSEs.

1. Three-body system

The Bethe-Salpeter amplitude $\Gamma(\{p_i\})$ for a three-body system shown in Fig. 8 depends on three momenta p_1, p_2, p_3 , whose sum is the total onshell momentum P with $P^2 = -M_B^2$. The three-body BSE is the covariant Faddeev equation and can be written as

$$\begin{aligned} \Gamma(\{p_i\}) &= \sum_a^3 \Gamma_{(a)}(\{p_i\}). \\ \Gamma_{(a)}(\{p_i\}) &= \int \frac{d^4 r}{(2\pi)^4} K(p_{a_1}, q_{a_1}, p_{a_2}, q_{a_2}) \\ &\quad \times D(q_{a_1}) D(q_{a_2}) \Gamma(\{p_i\}, a). \end{aligned} \quad (\text{A2})$$

In this case there are three possible two-body kernels $K_a \in \{K_{12}, K_{13}, K_{23}\}$, whose sum does not lead to overcounting in the three-body scattering matrix $T^{(3)}$. The amplitudes $\Gamma(\{p_i\}, a)$ inside the loop follow from $\Gamma(\{p_i\})$ with the replacements $p_{a_1} \rightarrow q_{a_1}$ and $p_{a_2} \rightarrow q_{a_2}$.

In practice it is useful to employ the solution strategy from Appendix C of Ref. [48], which takes advantage of the permutation-group properties of the amplitude and reduces the numerical effort considerably. Here only one of the diagrams in Fig. 8 needs to be calculated explicitly and the remaining ones are obtained by permutations,

$$\Gamma(\{p_i\}) = \Gamma_{(12)}(\{p_i\}) + \Gamma_{(12)}(\{p'_i\}) + \Gamma_{(12)}(\{p''_i\}), \quad (\text{A3})$$

where p'_i and p''_i are the respective permuted momenta. Instead of the three particle momenta p_i , it is also useful to work with the relative momenta q and p :

$$\begin{aligned} q &= \frac{p_2 - p_1}{2}, & p_1 &= -q - \frac{p}{2} + \frac{1-\eta}{2}P, \\ p &= (1-\eta)p_3 - \eta(p_1 + p_2), & p_2 &= q - \frac{p}{2} + \frac{1-\eta}{2}P, \\ P &= p_1 + p_2 + p_3, & p_3 &= p + \eta P, \end{aligned} \quad (\text{A4})$$

with $\eta = 1/3$ for equal masses. The resulting permuted relative momenta read

$$p' = -q - \frac{p}{2}, \quad p'' = q - \frac{p}{2}, \quad (\text{A5})$$

$$q' = -\frac{q}{2} + \frac{3p}{4}, \quad q'' = -\frac{q}{2} - \frac{3p}{4}. \quad (\text{A6})$$

We then solve the BSE amplitude for the variables $p^2, q^2, p \cdot q, p \cdot P$ and $q \cdot P$, which we expand in Chebyshev and Legendre polynomials. This is what we refer to as ‘full solution’ in the main text.

Like in the five-body system, we furthermore employ a singlet \times pole approximation

$$\Gamma(q, p, P) \approx f(\mathcal{S}_0) \sum_a \mathcal{P}_a. \quad (\text{A7})$$

Here the two-body pole for $a = 12$ is given by

$$\mathcal{P}_{12} = \frac{1}{(p_1 + p_2)^2 + M_M^2}, \quad (\text{A8})$$

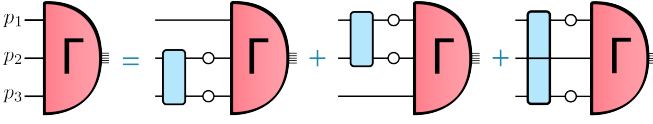


FIG. 8. Three-body BSE (A2) with two-body kernels.

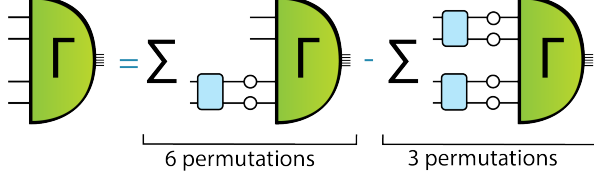


FIG. 9. Four-body BSE (A12) with two-body kernels and their counterterms.

with M_M the mass of the two-body subsystem or ‘di-quark’, and the singlet variable \mathcal{S}_0 is

$$\mathcal{S}_0 = \frac{q^2}{3} + \frac{p^2}{4}. \quad (\text{A9})$$

Finally, in the singlet approximation we reduce the momentum dependence to \mathcal{S}_0 by setting $\Gamma(q, p, P) \approx f(\mathcal{S}_0)$.

2. Four-body system

In the four-body BSE shown in Fig. 9, one encounters the same situation discussed in Sec. II B: A naive summation of two-body kernels leads to overcounting, and one needs subtraction terms [44–46]. In this case there are six possible two-body kernels

$$K_a \in \{K_{12}, K_{13}, K_{14}, K_{23}, K_{24}, K_{34}\} \quad (\text{A10})$$

and three independent double-kernel configurations of the form

$$K_a K_b \in \{K_{12} K_{34}, K_{13} K_{24}, K_{14} K_{23}\}. \quad (\text{A11})$$

The four-body Bethe-Salpeter amplitude $\Gamma(\{p_i\})$ depends on four-momenta $p_1 \dots p_4$, whose sum is the total onshell momentum P with $P^2 = -M_T^2$ (T for ‘tetra’). The four-body equation is the Faddeev-Yakubowski equation and can be written as

$$\begin{aligned} \Gamma(\{p_i\}) &= \sum_a^6 \Gamma_{(a)}(\{p_i\}) - \sum_{a \neq b}^3 \Gamma_{(a,b)}(\{p_i\}), \\ \Gamma_{(a)}(\{p_i\}) &= \int \frac{d^4 r}{(2\pi)^4} K(p_{a_1}, q_{a_1}, p_{a_2}, q_{a_2}) \\ &\quad \times D(q_{a_1}) D(q_{a_2}) \Gamma(\{p_i\}, a), \\ \Gamma_{(a,b)}(\{p_i\}) &= \int \frac{d^4 r}{(2\pi)^4} K(p_{a_1}, q_{a_1}, p_{a_2}, q_{a_2}) \\ &\quad \times D(q_{a_1}) D(q_{a_2}) \Gamma_{(b)}(\{p_i\}, a), \end{aligned} \quad (\text{A12})$$

where the amplitudes $\Gamma(\{p_i\}, a)$ inside the loop follow from $\Gamma(\{p_i\})$ with the replacements $p_{a_1} \rightarrow q_{a_1}$ and $p_{a_2} \rightarrow q_{a_2}$. In practice it is useful to work with the total momentum P and the three relative momenta p, q, k instead of the particle momenta p_i with $i = 1 \dots 4$. To this end, we employ the Jacobi momenta

$$\begin{aligned} p_1 &= \frac{k + q - p}{2} + \frac{P}{4}, & p_3 &= \frac{-k + p + q}{2} + \frac{P}{4}, \\ p_2 &= \frac{k - q + p}{2} + \frac{P}{4}, & p_4 &= -\frac{k + p + q}{2} + \frac{P}{4}. \end{aligned} \quad (\text{A13})$$

Applying the same solution strategy as in the three-body case discussed above, we relate all amplitudes on the r.h.s. of Fig. 9 to one diagram through permutations. This also applies to the double-kernel diagrams, which can be obtained by multiplying the kernel onto the respective amplitude once more.

In the four-body case, a full solution without any restrictions on the amplitude is numerically not feasible, so we employ the singlet \times pole approximation [13, 54, 55]

$$\Gamma(q, p, k, P) \approx f(\mathcal{S}_0) \sum_a \mathcal{P}_{aa'}, \quad (\text{A14})$$

where the two-body poles for $aa' = (12)(34)$ are given by

$$\mathcal{P}_{(12)(34)} = \frac{1}{(p_1 + p_2)^2 + M_M^2} \frac{1}{(p_3 + p_4)^2 + M_M^2} \quad (\text{A15})$$

and M_M is the mass of the two-body subsystem. The singlet variable \mathcal{S}_0 is

$$\mathcal{S}_0 = \frac{k^2 + q^2 + p^2}{4}. \quad (\text{A16})$$

In the singlet approximation, we further reduce the momentum dependence to \mathcal{S}_0 via $\Gamma(q, p, k, P) \approx f(\mathcal{S}_0)$.

3. Five-body system

The five-body BSE has already been discussed in the main text, Eqs. (18–24). Its solution proceeds along the same lines as for the two- and three-body BSEs. We employ the singlet \times pole approximation (25) and relate all terms in the BSE to one diagram such that

$$\Gamma_{(a)}(\{p_i\}) = \Gamma_{(12)}(\{p_i^{(a)}\}), \quad (\text{A17})$$

where the $p_i^{(a)}$ are the permuted four-momenta.

Furthermore, as discussed in Appendix D of Ref. [43], for a five-body system one encounters for the first time a dimensional constraint relating the Lorentz invariants in Eq. (23). Therefore, a singlet approximation where all variables except \mathcal{S}_0 are set to zero is, strictly speaking, not possible because in that case also \mathcal{S}_0 would vanish. To this end, we keep one of the variables η_i from Eq. (23) in the system but set it to a fixed value, so that the amplitude still depends only on \mathcal{S}_0 . The singlet approximation in the five-body case is then analogous to the three- and four-body systems.

-
- [1] R. Aaij *et al.* (LHCb), Observation of $J/\psi p$ Resonances Consistent with Pentaquark States in $\Lambda_b^0 \rightarrow J/\psi K^- p$ Decays, *Phys. Rev. Lett.* **115**, 072001 (2015), [arXiv:1507.03414 \[hep-ex\]](#).
- [2] R. Aaij *et al.* (LHCb), Observation of a narrow pentaquark state, $P_c(4312)^+$, and of two-peak structure of the $P_c(4450)^+$, *Phys. Rev. Lett.* **122**, 222001 (2019), [arXiv:1904.03947 \[hep-ex\]](#).
- [3] R. Aaij *et al.* (LHCb), Observation of a $J/\psi \Lambda$ Resonance Consistent with a Strange Pentaquark Candidate in $B \rightarrow J/\psi \Lambda p^-$ Decays, *Phys. Rev. Lett.* **131**, 031901 (2023), [arXiv:2210.10346 \[hep-ex\]](#).
- [4] H.-X. Chen, W. Chen, X. Liu, and S.-L. Zhu, The hidden-charm pentaquark and tetraquark states, *Phys. Rept.* **639**, 1 (2016), [arXiv:1601.02092 \[hep-ph\]](#).
- [5] R. F. Lebed, R. E. Mitchell, and E. S. Swanson, Heavy-Quark QCD Exotica, *Prog. Part. Nucl. Phys.* **93**, 143 (2017), [arXiv:1610.04528 \[hep-ph\]](#).
- [6] A. Esposito, A. Pilloni, and A. D. Polosa, Multiquark Resonances, *Phys. Rept.* **668**, 1 (2017), [arXiv:1611.07920 \[hep-ph\]](#).
- [7] F.-K. Guo, C. Hanhart, U.-G. Meißner, Q. Wang, Q. Zhao, and B.-S. Zou, Hadronic molecules, *Rev. Mod. Phys.* **90**, 015004 (2018), [Erratum: *Rev. Mod. Phys.* **94**, 029901 (2022)], [arXiv:1705.00141 \[hep-ph\]](#).
- [8] A. Ali, J. S. Lange, and S. Stone, Exotics: Heavy Pentaquarks and Tetraquarks, *Prog. Part. Nucl. Phys.* **97**, 123 (2017), [arXiv:1706.00610 \[hep-ph\]](#).
- [9] Y.-R. Liu, H.-X. Chen, W. Chen, X. Liu, and S.-L. Zhu, Pentaquark and Tetraquark states, *Prog. Part. Nucl. Phys.* **107**, 237 (2019), [arXiv:1903.11976 \[hep-ph\]](#).
- [10] N. Brambilla, S. Eidelman, C. Hanhart, A. Nefediev, C.-P. Shen, C. E. Thomas, A. Vairo, and C.-Z. Yuan, The XYZ states: experimental and theoretical status and perspectives, *Phys. Rept.* **873**, 1 (2020), [arXiv:1907.07583 \[hep-ex\]](#).
- [11] G. Eichmann, C. S. Fischer, and W. Heupel, The light scalar mesons as tetraquarks, *Phys. Lett. B* **753**, 282 (2016), [arXiv:1508.07178 \[hep-ph\]](#).
- [12] G. Eichmann, C. S. Fischer, W. Heupel, N. Santowsky, and P. C. Wallbott, Four-Quark States from Functional Methods, *Few Body Syst.* **61**, 38 (2020), [arXiv:2008.10240 \[hep-ph\]](#).
- [13] J. Hoffer, G. Eichmann, and C. S. Fischer, Hidden-flavor four-quark states in the charm and bottom region, *Phys. Rev. D* **109**, 074025 (2024), [arXiv:2402.12830 \[hep-ph\]](#).
- [14] G. Eichmann, H. Sanchis-Alepuz, R. Williams, R. Alkofer, and C. S. Fischer, Baryons as relativistic three-quark bound states, *Prog. Part. Nucl. Phys.* **91**, 1 (2016), [arXiv:1606.09602 \[hep-ph\]](#).
- [15] M. Y. Barabanov *et al.*, Diquark correlations in hadron physics: Origin, impact and evidence, *Prog. Part. Nucl. Phys.* **116**, 103835 (2021), [arXiv:2008.07630 \[hep-ph\]](#).
- [16] E. E. Salpeter and H. A. Bethe, A Relativistic equation for bound state problems, *Phys. Rev.* **84**, 1232 (1951).
- [17] M. Gell-Mann and F. Low, Bound states in quantum field theory, *Phys. Rev.* **84**, 350 (1951).
- [18] J. S. Schwinger, On the Green's functions of quantized fields. 1., *Proc. Nat. Acad. Sci.* **37**, 452 (1951).
- [19] F. J. Dyson, The S matrix in quantum electrodynamics, *Phys. Rev.* **75**, 1736 (1949).
- [20] G. C. Wick, Properties of Bethe-Salpeter Wave Functions, *Phys. Rev.* **96**, 1124 (1954).
- [21] R. E. Cutkosky, Solutions of a Bethe-Salpeter equations, *Phys. Rev.* **96**, 1135 (1954).
- [22] N. Nakanishi, A General survey of the theory of the Bethe-Salpeter equation, *Prog. Theor. Phys. Suppl.* **43**, 1 (1969).
- [23] F. L. Scarf, Spectrum and nonrelativistic limit of a bethe-salpeter equation, *Phys. Rev.* **100**, 912 (1955).
- [24] N. Nakanishi, Partial-Wave Bethe-Salpeter Equation, *Phys. Rev.* **130**, 1230 (1963).
- [25] N. Nakanishi, Review of the Wick-cutkosky Model, *Prog. Theor. Phys. Suppl.* **95**, 1 (1988).
- [26] N. Seto and I. Fukui, Scalar scalar ladder model in the unequal mass case. 1: Numerical evidence for the complex eigenvalues, *Prog. Theor. Phys.* **89**, 205 (1993).
- [27] I. Fukui and N. Seto, Scalar-scalar ladder model in the unequal mass case. 2. Numerical studies of the BS amplitudes, *Prog. Theor. Phys.* **95**, 433 (1996), [arXiv:hep-ph/9509382](#).
- [28] K. Kusaka and A. G. Williams, Solving the Bethe-Salpeter equation for scalar theories in Minkowski space, *Phys. Rev. D* **51**, 7026 (1995), [arXiv:hep-ph/9501262](#).
- [29] T. Nieuwenhuis and J. A. Tjon, $O(4)$ expansion of the ladder Bethe-Salpeter equation, *Few Body Syst.* **21**, 167 (1996), [arXiv:nucl-th/9607041](#).
- [30] K. Kusaka, K. M. Simpson, and A. G. Williams, Solving the Bethe-Salpeter equation for bound states of scalar theories in Minkowski space, *Phys. Rev. D* **56**, 5071 (1997), [arXiv:hep-ph/9705298](#).
- [31] S. Ahlig and R. Alkofer, (In)consistencies in the relativistic description of excited states in the Bethe-Salpeter equation, *Annals Phys.* **275**, 113 (1999), [arXiv:hep-th/9810241](#).
- [32] V. Sauli and J. Adam, Jr., Study of relativistic bound states for scalar theories in the Bethe-Salpeter and Dyson-Schwinger formalism, *Phys. Rev. D* **67**, 085007 (2003), [arXiv:hep-ph/0111433](#).
- [33] V. A. Karmanov and J. Carbonell, Solving Bethe-Salpeter equation in Minkowski space, *Eur. Phys. J. A* **27**, 1 (2006), [arXiv:hep-th/0505261](#).
- [34] T. Frederico, G. Salme, and M. Viviani, Two-body scattering states in Minkowski space and the Nakanishi integral representation onto the null plane, *Phys. Rev. D* **85**, 036009 (2012), [arXiv:1112.5568 \[hep-ph\]](#).
- [35] T. Frederico, G. Salme, and M. Viviani, Quantitative studies of the homogeneous Bethe-Salpeter Equation in Minkowski space, *Phys. Rev. D* **89**, 016010 (2014), [arXiv:1312.0521 \[hep-ph\]](#).
- [36] C. Gutierrez, V. Gigante, T. Frederico, G. Salmè, M. Viviani, and L. Tomio, Bethe-Salpeter bound-state structure in Minkowski space, *Phys. Lett. B* **759**, 131 (2016), [arXiv:1605.08837 \[hep-ph\]](#).
- [37] G. Eichmann, P. Duarte, M. T. Peña, and A. Stadler, Scattering amplitudes and contour deformations, *Phys. Rev. D* **100**, 094001 (2019), [arXiv:1907.05402 \[hep-ph\]](#).
- [38] G. Eichmann, E. Ferreira, and A. Stadler, Going to the light front with contour deformations, *Phys. Rev. D* **105**, 034009 (2022), [arXiv:2112.04858 \[hep-ph\]](#).
- [39] F. Fornetti, A. Gnech, T. Frederico, F. Pederiva, M. Rinaldi, A. Roggero, G. Salme', S. Scopetta, and M. Vi-

- viani, Solving the homogeneous Bethe-Salpeter equation with a quantum annealer, *Phys. Rev. D* **110**, 056012 (2024), [arXiv:2406.18669 \[hep-ph\]](#).
- [40] V. A. Karmanov and P. Maris, Manifestation of three-body forces in three-body Bethe-Salpeter and light-front equations, *Few Body Syst.* **46**, 95 (2009), [arXiv:0811.1100 \[hep-ph\]](#).
- [41] E. Ydrefors, J. H. Alvarenga Nogueira, V. Gigante, T. Frederico, and V. A. Karmanov, Three-body bound states with zero-range interaction in the Bethe-Salpeter approach, *Phys. Lett. B* **770**, 131 (2017), [arXiv:1703.07981 \[nucl-th\]](#).
- [42] E. Ydrefors, J. H. Alvarenga Nogueira, V. A. Karmanov, and T. Frederico, Solving the three-body bound-state Bethe-Salpeter equation in Minkowski space, *Phys. Lett. B* **791**, 276 (2019), [arXiv:1903.01741 \[hep-ph\]](#).
- [43] G. Eichmann and R. D. Torres, Five-point functions and the permutation group S_5 , (2025), [arXiv:2502.17225 \[hep-ph\]](#).
- [44] K. Huang and H. A. Weldon, Bound-state wave functions and bound-state scattering in relativistic field theory, *Physical Review D* **11**, 257 (1975).
- [45] A. N. Kvinikhidze and A. M. Khvedelidze, Pair-interaction approximation in the equations of quantum field theory for a four-body system, *Theoretical and Mathematical Physics* **90**, 62 (1992).
- [46] W. Heupel, G. Eichmann, and C. S. Fischer, Tetraquark Bound States in a Bethe-Salpeter Approach, *Phys. Lett. B* **718**, 545 (2012), [arXiv:1206.5129 \[hep-ph\]](#).
- [47] G. Eichmann, R. Williams, R. Alkofer, and M. Vujanovic, Three-gluon vertex in Landau gauge, *Phys. Rev. D* **89**, 105014 (2014), [arXiv:1402.1365 \[hep-ph\]](#).
- [48] G. Eichmann, Nucleon electromagnetic form factors from the covariant Faddeev equation, *Phys. Rev. D* **84**, 014014 (2011), [arXiv:1104.4505 \[hep-ph\]](#).
- [49] G. Eichmann, C. S. Fischer, and W. Heupel, Four-point functions and the permutation group S_4 , *Phys. Rev. D* **92**, 056006 (2015), [arXiv:1505.06336 \[hep-ph\]](#).
- [50] F. Pinto-Gómez, F. De Soto, M. N. Ferreira, J. Papavasiliou, and J. Rodríguez-Quintero, Lattice three-gluon vertex in extended kinematics: Planar degeneracy, *Phys. Lett. B* **838**, 137737 (2023), [arXiv:2208.01020 \[hep-ph\]](#).
- [51] M. N. Ferreira and J. Papavassiliou, Gauge Sector Dynamics in QCD, *Particles* **6**, 312 (2023), [arXiv:2301.02314 \[hep-ph\]](#).
- [52] A. C. Aguilar, M. N. Ferreira, J. Papavassiliou, and L. R. Santos, Planar degeneracy of the three-gluon vertex, *Eur. Phys. J. C* **83**, 549 (2023), [arXiv:2305.05704 \[hep-ph\]](#).
- [53] A. C. Aguilar, M. N. Ferreira, J. Papavassiliou, and L. R. Santos, Four-gluon vertex in collinear kinematics, *Eur. Phys. J. C* **84**, 676 (2024), [arXiv:2402.16071 \[hep-ph\]](#).
- [54] P. C. Wallbott, G. Eichmann, and C. S. Fischer, $X(3872)$ as a four-quark state in a Dyson-Schwinger/Bethe-Salpeter approach, *Phys. Rev. D* **100**, 014033 (2019), [arXiv:1905.02615 \[hep-ph\]](#).
- [55] P. C. Wallbott, G. Eichmann, and C. S. Fischer, Disentangling different structures in heavy-light four-quark states, *Phys. Rev. D* **102**, 051501 (2020), [arXiv:2003.12407 \[hep-ph\]](#).
- [56] G. Eichmann, A. Gómez, J. Horak, J. M. Pawłowski, J. Wessely, and N. Wink, Bound states from the spectral Bethe-Salpeter equation, *Phys. Rev. D* **109**, 096024 (2024), [arXiv:2310.16353 \[hep-ph\]](#).
- [57] R. Lehoucq, D. Sorensen, and C. Yang, Arpack users' guide, Society for Industrial and Applied Mathematics (1998).
- [58] N. Santowsky, G. Eichmann, C. S. Fischer, P. C. Wallbott, and R. Williams, σ -meson: Four-quark versus two-quark components and decay width in a Bethe-Salpeter approach, *Phys. Rev. D* **102**, 056014 (2020), [arXiv:2007.06495 \[hep-ph\]](#).